Research Article | Vol. 6, No. 10 | 1 Oct 2016 | OPTICAL MATERIALS EXPRESS 3366

Optical Materials EXPRESS

Investigation of the optical properties of $LiTi_2O_4$ and $Li_4Ti_5O_{12}$ spinel films by spectroscopic ellipsometry

MINGLIN ZHAO,[1] JIE LIAN,[1,*] YANLI JIA,[2] KUI JIN,[2] LIPING XU,[3] ZHIGAO HU,[3] XIULUN YANG,[1] AND SHISHOU KANG[4]

[1]*School of Information Science and Engineering, Shandong University, Jinan 250100, Shandong, China*
[2]*National Lab for Superconductivity, Institute of Physics, Chinese Academy of Sciences, Beijing 100190, China*
[3]*Key Laboratory of Polar Materials and Devices, Ministry of Education, East China Normal University, Shanghai 200241, China*
[4]*School of Physics, Shandong University, Jinan 250100, Shandong, China*
**jieliansdu@163.com*

Abstract: The spinel lithium titanates materials $Li_4Ti_5O_{12}$ and $LiTi_2O_4$ were fabricated by pulsed laser deposition. High quality and single phase thin films were successfully grown, thus opening the door for a systematic investigation of the optical properties of the spinel system $Li_{1+x}Ti_{2-x}O_4$ ($0 \leq x \leq 1/3$). The microstructure of $Li_{1+x}Ti_{2-x}O_4$ films were characterized by X-ray diffraction and atomic force microscope. The optical properties of the films were studied by spectroscopic ellipsometry at room temperature. The refractive index, extinction coefficient, and the thickness of the films were obtained by fitting the experimental data over the entire measured wavelength range. The results show that the two spinel oxides exhibit absolutely different dispersion trends in the visible region. The optical band gap of $Li_4Ti_5O_{12}$ is about 3.14eV. The crystal-field energy splitting of $LiTi_2O_4$ is about 2.09eV between the e_g and the t_{2g} orbitals.

OCIS codes: (160.4760) Optical properties; (310.6860) Thin films, optical properties; (160.4670) Optical materials; (240.2130) Ellipsometry and polarimetry.

References and links

1. Y. Moritomo, Sh. Xu, A. Machida, T. Akimoto, E. Nishibori, M. Takata, and M. Sakata, "Electronic structure of double-perovskite transition-metal oxides," Phys. Rev. B **61**(12), R7827–R7830 (2000).
2. D. C. Johnston, "Superconducting and normal state properties of Li_{1+x} Ti_{2-x} O_4 spinel compounds. I. Preparation, crystallography, superconducting properties, electrical resistivity, dielectric behavior, and magnetic susceptibility," J. Low Temp. Phys. **25**(1-2), 145–175 (1976).
3. R. N. Bhowmik and R. Ranganathan, "Magnetic order and electrical conductivity scaling of the spinel oxide $Mn_{0.5}Ru_{0.5}Co_2O_4$," Phys. Rev. B **74**(21), 214417 (2006).
4. E. Dagotto, "Complexity in strongly correlated electronic systems," Science **309**(5732), 257–262 (2005).
5. D. C. Johnston, H. Prakash, W. H. Zachariasen, and R. Viswanathan, "High temperature superconductivity in the $Li_{1+x}Ti_{2-x}O_4$ ternary system," Mater. Res. Bull. **8**(7), 777–784 (1973).
6. S. Maruyama, J. Shin, X. Zhang, R. Suchoski, S. Yasui, K. Jin, R. L. Greene, and I. Takeuchi, "Reversible electrochemical modulation of the superconducting transition temperature of $LiTi_2O_4$ ultrathin films by ionic liquid gating," Appl. Phys. Lett. **107**(14), 142602 (2015).
7. K. Jin, G. He, X. Zhang, S. Maruyama, S. Yasui, R. Suchoski, J. Shin, Y. Jiang, H. S. Yu, J. Yuan, L. Shan, F. V. Kusmartsev, R. L. Greene, and I. Takeuchi, "Anomalous magnetoresistance in the spinel superconductor $LiTi_2O_4$," Nat. Commun. **6**, 7183 (2015).
8. T. Ohzuku, A. Ueda, and N. Yamamoto, "Zero-strain insertion material of Li $[Li_{1/3}Ti_{5/3}]$ O_4 for Rechargeable Lithium Cells," J. Electrochem. Soc. **142**(5), 1431–1435 (1995).
9. A. Guerfia, S. Sévignya, M. Lagacéa, P. Hovingtona, K. Kinoshitab, and K. Zaghiba, "Nano-particle $Li_4Ti_5O_{12}$ spinel as electrode for electrochemical generators," J. Power Sources **119**, 88–94 (2003).
10. K. Amine, I. Belharouak, Z. Chen, T. Tran, H. Yumoto, N. Ota, S. T. Myung, and Y. K. Sun, "Nanostructured anode material for high-power battery system in electric vehicles," Adv. Mater. **22**(28), 3052–3057 (2010).
11. M. R. Harrison, P. P. Edwards, and J. B. Goodenough, "The superconductor-semiconductor transition in the $Li_{1+x}Ti_{2-x}O_4$ spinel system," Philos. Mag. B **52**(3), 679–699 (1985).

#273236 http://dx.doi.org/10.1364/OME.6.003366
Journal © 2016 Received 4 Aug 2016; revised 15 Sep 2016; accepted 22 Sep 2016; published 30 Sep 2016

Optical Materials EXPRESS

12. M. Dalton, I. Gameson, A. R. Armstrong, and P. P. Edwards, "Structure of the $Li_{1+x}Ti_{2-x}O_4$ superconducting system: A neutron diffraction study," Physica C **221**(1-2), 149–156 (1994).
13. M. Ýapinski, B. Kościelska, A. Winiarski, and W. Sadowski, "XPS study of superconducting $LiTi_2O_4$ and $LiTi_{2-x}Cu_xO_4$ Sol-Gel derived powders and thin films," Acta Phys. Pol. A **126**, 107–109 (2014).
14. W. Ra, M. Nakayama, Y. Uchimoto, and M. Wakihara, "Experimental and computational study of the electronic structural changes in $LiTi_2O_4$ spinel compounds upon electrochemical Li insertion reactions," J. Phys. Chem. B **109**(3), 1130–1134 (2005).
15. M. Xiangdong, W. Xiaocen, Z. Yuxue, T. Ling, Z. Xianghua, and C. Xiaobing, "Spinel lithium titanate from brookite nanocrystallites," Ceram. Int. **40**(3), 4989–4993 (2014).
16. A. Kumatani, T. Ohsawa, R. Shimizu, Y. Takagi, S. Shiraki, and T. Hitosugi, "Growth processes of lithium titanate thin films deposited by using pulsed laser deposition," Appl. Phys. Lett. **101**(12), 123103 (2012).
17. T. Inukai, T. Murakami, and T. Inamura, "Preparation of superconducting $LiTi_2O_4$ thin films," Thin Solid Films **94**(1), 47–50 (1982).
18. L. Tang, P. Y. Zou, L. Shan, A. F. Dong, G. C. Che, and H. H. Wen, "Electrical resistivity and Andreev re□ection spectroscopy of the superconducting oxide spinel $LiTi_2O_4$," Phys. Rev. B **73**(18), 184521 (2006).
19. J. Mosaa, M. Aparicioa, K. Tadanagab, A. Hayashib, and M. Tatsumisagob, "$Li_4Ti_5O_{12}$ thin-film electrodes by in-situ synthesis of lithium alkoxide for Li-ion microbatteries," Electrochim. Acta **149**, 293–299 (2014).
20. S. Özen, V. Şenay, S. Pat, and Ş. Korkmaz, "Optical, morphological properties and surface energy of the transparent $Li_4Ti_5O_{12}$ (LTO) thin film as anode material for secondary type batteries," J. Phys. D Appl. Phys. **49**(10), 105303 (2016).
21. V. Miikkulainen, O. Nilsen, M. Laitinen, T. Sajavaara, and H. Fjellvåg, "Atomic layer deposition of $Li_xTi_yO_z$ thin films," RSC Advances **3**(20), 7537–7542 (2013).
22. Y. L. Jia and G. He, *et al*., "Crystallographic dependent transport properties and oxygen issue in superconducting $LiTi_2O_4$ thin films," http://arxiv.org/abs/1608.06683.
23. J. I. Pankove, Optical Processes in Semiconductors (Dover, 1971).
24. C. Y. Ouyang, Z. Y. Zhong, and M. S. Lei, "Ab initio studies of structural and electronic properties of $Li_4Ti_5O_{12}$ spinel," Electrochem. Commun. **9**(5), 1107–1112 (2007).
25. D. T. Liu, C. Y. Ouyang, J. Shu, J. Jiang, Z. X. Wang, and L. Q. Chen, "Theoretical study of cation doping effect on the electronic conductivity of $Li_4Ti_5O_{12}$," Phys. Status Solidi, B Basic Res. **243**(8), 1835–1841 (2006).
26. K. Kanamura, T. Umegak, H. Naito, Z. Takehara, and T. Yao, "Structural and electrochemical characteristics of $Li_{4/3}Ti_{5/3}O_4$ as an anode material for rechargeable lithium batteries," J. Appl. Electrochem. **31**(1), 73–78 (2001).
27. Y. R. Jhan and J. G. Duh, "Electrochemical performance and low discharge cut-off voltage behavior of ruthenium doped $Li_4Ti_5O_{12}$ with improved energy density," Electrochim. Acta **63**, 9–15 (2012).
28. H. Duan, J. Li, S. W. Chiang, H. Du, and W. H. Duan, "First-principles study of native defects in $LiTi_2O_4$," Comput. Mater. Sci. **96**, 263–267 (2015).
29. S. Satpathy and R. M. Martin, "Electronic structure of the superconducting oxide spinel $LiTi_2O_4$," Phys. Rev. B **36**(13), 7269–7272 (1987).
30. S. Massidda, J. Yu, and A. J. Freeman, "Electronic structure and properties of superconducting $LiTi_2O_4$.," Phys. Rev. B Condens. Matter **38**(16), 11352–11357 (1988).
31. W. Ra, M. Nakayama, Y. Uchimoto, and M. Wakihara, "Experimental and Computational Study of the Electronic Structural Changes in $LiTi_2O_4$ Spinel Compounds upon Electrochemical Li Insertion Reactions," J. Phys. Chem. B **109**(3), 1130–1134 (2005).
32. W. F. J. Fontijn, P. J. van der Zaag, L. F. Feiner, R. Metselaar, and M. A. C. Devillers, "A consistent interpretation of the magneto-optical spectra of spinel type ferrites (invited)," J. Appl. Phys. **85**(8), 5100–5105 (1999).
33. J. S. Griffith, *The Theory of Transition Metal Ions* (Cambridge University Press, 1971).
34. K. J. Kim and J. H. Lee, "Effects of nickel doping on structural and optical properties of spinel lithium manganate thin films," Solid State Commun. **141**(2), 99–103 (2007).

1. Introduction

Transition-metal oxides crystallizing in the spinel structure have generated great interest due to rich physical phenomena such as high-temperature superconductor, ferrimagnetism, metal-insulator transition and so on [1–4]. As one of those transition metal oxides, the spinel system $Li_{1+x}Ti_{2-x}O_4$ ($0 \leq x \leq 1/3$) has attracted much attention following the discovery by Johnston et al [5]. The initial member $LiTi_2O_4$, the only known oxide spinel superconductor, has a superconducting transition temperature (T_c) of 13.7K for bulk materials [5] and display T_c of about 11K for thin films [6,7]. The ending member $Li_4Ti_5O_{12}$ is a most promising anode material for Li-ion battery due to its high reaction rate of lithium insertion and extraction [8–10]. The disappearance of superconductivity with increasing x is correlated with anomalous changes in the lattice parameter with composition and is attributed to the occurrence of a composition-induced metal-semiconductor transition at $x \approx 0.1$ from electrical resistivity

Optical Materials EXPRESS

measurements [2].The metal-semiconductor transition is due to a disproportionation into Li-rich and Li-poor compositions at the grain boundaries [11]. Dalton et al [12] suggested that all members of $Li_{1+x}Ti_{2-x}O_4$ (LTO) have a cubic symmetry with the space group of Fd3m, where the 8a tetrahedral positions are occupied entirely by lithium ions whereas the 16d octahedral sites are randomly occupied by (x) lithium ions and (2-x) titanium ions per formula unit. LTO films were produced by means of various techniques, such as solid-state reaction, thermal processes, sol-gel method, RF magnetron sputtering method and pulsed laser deposition [13–17], and mostly LTO films are utilized in polycrystalline forms [18]. The thermal, electrical and magnetic properties have been extensively investigated for decades. However, the optical research reports of LTO films are few, due to the lack of the single crystals and high quality thin films. In recent years, some researches have been reported on optical properties of $Li_4Ti_5O_{12}$ [19–21]. But the analysis on the optical properties of $LiTi_2O_4$ film still remain unreported. We have successfully grown high quality single crystalline-like epitaxial LTO thin films. Thus, we could systematic investigate and contrast the optical properties of the two kinds of $Li_{1+x}Ti_{2-x}O_4$ films for the first time.

In the present paper, LTO thin films were prepared by pulsed laser deposition (PLD) on $MgAl_2O_4$ (001) substrates. X-ray diffraction (XRD) and atomic force microscopy (AFM) were performed to characterize the microstructure and the surface morphology of the films. We report on ellipsometric measurements of the LTO films in the visible region. Cauchy dispersion function and Drude-Lorentz dispersion function were succesfully used to describe the optical properties of $Li_4Ti_5O_{12}$ and $LiTi_2O_4$, respectively. The optical interband transitions of $LiTi_2O_4$ have been explicated. The results show that the optical properties of the two LTO films are absolutely different.

2. Experimental method

The $Li_4Ti_5O_{12}$ and $LiTi_2O_4$ thin films were epitaxially grown on (001)-oriented $MgAl_2O_4$ substrates via pulsed laser deposition technique in an ultrahigh-vacuum chamber. By controlling the oxygen partial pressure during deposition, we obtained the two end members of the spinel-phase system $Li_{1+x}Ti_{2-x}O_4$ ($0 \le x \le 1/3$) from a single target. The details of the preparation of the thin films can be found elsewhere [6,7,22]. That is, starting with a Li:Ti ratio of 4:5 in the target, a ratio of 1:2 is obtained in the film at low oxygen partial pressures. This effect is discussed in Ref. 16. The $LiTi_2O_4$ thin film used in this study show T_c of ~11K with narrow transition widths of <0.5K. The microstructure analyses of the films were carried out by X-ray diffraction (D8 Advance, Bruker AXS with Cu-Kα radiation). The surface morphology was analysed by atomic force microscope (NaioAFM, Nanosurf, Switzerland) in taping mode.

Spectroscopic ellipsometry measurement of $Li_4Ti_5O_{12}$ was recorded with a GES5 Sopra made rotating polarizer spectroscopic ellipsometer, in the wavelength 300-800nm. The ellipsometric measurement of $LiTi_2O_4$ was carried out using ultraviolet–near infrared spectroscopic ellipsometry (V-VASE by J. A. Woollam, Inc.), in the wavelength 300-2500nm. All the spectra were taken at an angle of incidence (φ) of 75° and all the calculations were performed using the Winelli software. Ellipsometry does not directly measure the optical constants or the film thickness, but two ellipsometric angels, Δ and ψ. From the software Winelli, we can get $\tan(\psi)$ and $\cos(\Delta)$, as well as the ellipsometric parameters $\cos(2\psi)$ and $\sin(2\psi)\cos(\Delta)$, as output. These angles describe the amplitude and phase of the light, which were changed after reflection from a sample. This change is measured as the ratio $\rho\left(=r_p/r_s\right)$ of the p (parallel) and s (perpendicular) field components of the light beam defined with respect to the plane of incidence of the sample. The relation between ρ and the optical constants is given by:

Optical Materials EXPRESS

$$\rho = \tan(\psi)\exp(i\Delta) = \frac{r_{1p} + r_{2p}\exp(-i\delta)}{1 + r_{1p}r_{2p}\exp(-i\delta)} \times \frac{1 + r_{1s}r_{2s}\exp(-i\delta)}{r_{1s} + r_{2s}\exp(-i\delta)} = f(n_1, n_2, n, \lambda, d) \quad (1)$$

By assuming a suitable optical model of the films and finding the best match via a least-square fitting calculation, the optical constants of LTO films, which is the function of wavelength, can be determined.

3. Results and discussion

3.1 Microstructure analyses of the LTO

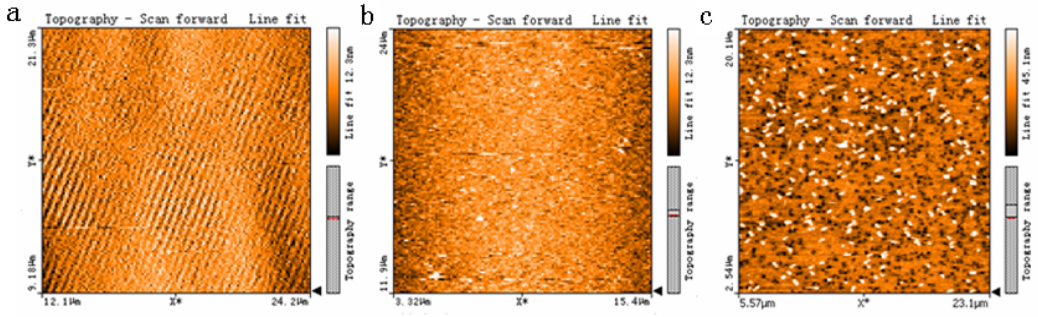

Fig. 1. 2D images of the LTO thin films and $MgAl_2O_4$ substrate surfaces performed by AFM, (a) $MgAl_2O_4$ substrate (b) $LiTi_2O_4$ thin film; (c) $Li_4Ti_5O_{12}$ thin film.

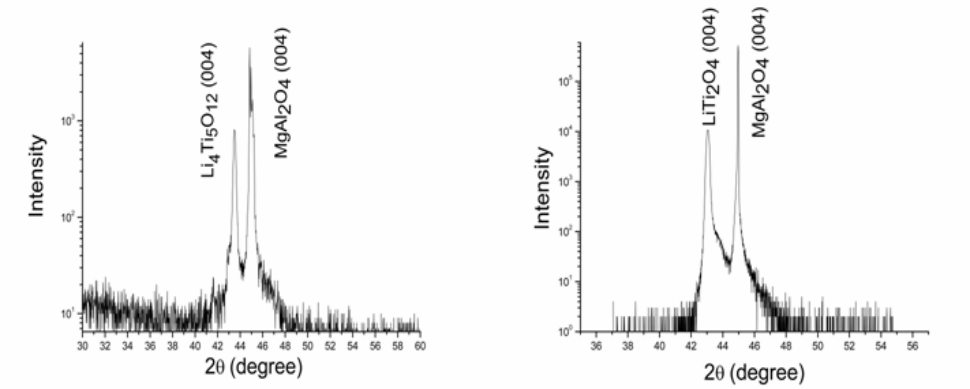

Fig. 2. XRD spectra (Cu Kα radiation = 1.5418 Å) of the LTO thin films grown on (001) $MgAl_2O_4$ substrate, Left: $Li_4Ti_5O_{12}$ thin film; Right: $LiTi_2O_4$ thin film.

The surface morphology of the $MgAl_2O_4$ substrate, $LiTi_2O_4$ thin film and $Li_4Ti_5O_{12}$ is shown in Fig. 1. Step and terrace structure is clearly observed in $MgAl_2O_4$ substrate. The grown $LiTi_2O_4$ thin film shows a rather smooth epitaxial thin film surface. While, rougher film morphology was seen in $Li_4Ti_5O_{12}$ thin film. As presented in Fig. 2, the XRD structure analysis indicated that both $LiTi_2O_4$ and $Li_4Ti_5O_{12}$ thin films were single phase, and the spinel phase reflections were epitaxially matched to the spinel single phase substrate. The full width at half maximum of (004) peaks for $LiTi_2O_4$ and $Li_4Ti_5O_{12}$ are about 0.142 degree and 0.181 degree, respectively, which reveals that both thin films exhibit good orientation. The XRD patterns of the two materials look similar, but the (004) peak of $LiTi_2O_4$ (2θ = 43.06°) clearly shifts to a lower 2θ angle compared with that of $Li_4Ti_5O_{12}$ (2θ = 43.48°). Which is due to the fact that spinel $LiTi_2O_4$ has a bulk room temperature lattice parameter of a = 8.405Å and $Li_4Ti_5O_{12}$ has a = 8.359Å, hence there is a larger compressive lattice mismatch with the spinel

Optical Materials EXPRESS

$MgAl_2O_4$ substrate (a = 8.08Å). As mentioned above, we can confirm that the quality of the two films is excellent.

3.2 Ellipsometry analysis of the LTO

Table 1. The best fitting parameters in Cauchy model for the $Li_4Ti_5O_{12}$ film.

	A	B	C	D	E	F
Cauchy	2.1123	0.0389	1.0275E-3	0.0181	5.0819E-3	–2.2582E-4

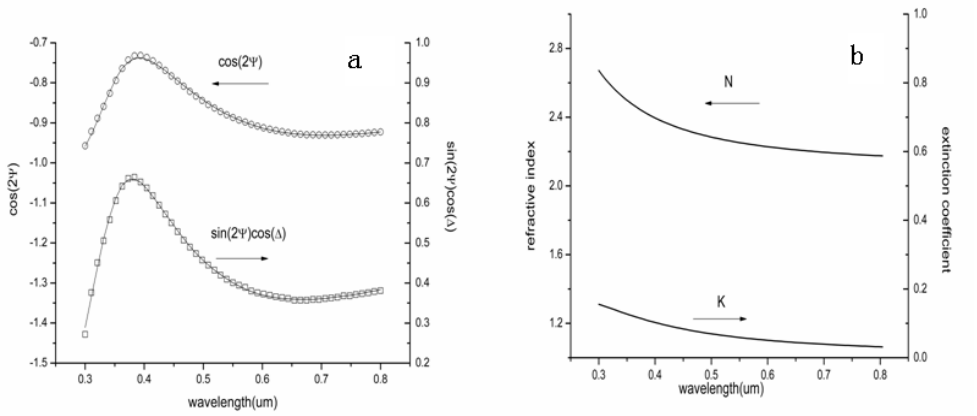

Fig. 3. (a) Measured (dotted) and fitted (lines) ellipsometric spectra cos(2 ψ) and sin(2 ψ)cos(Δ) of $Li_4Ti_5O_{12}$ thin film at the incident angle of 75° (b) Refractive index and extinction coefficient for $Li_4Ti_5O_{12}$ thin film.

The measured ellipsometric angles and corresponding fitting results of $Li_4Ti_5O_{12}$ thin film are shown in Fig. 3(a). According to the analysis of AFM, $Li_4Ti_5O_{12}$ thin film has a rougher surface. The ellipsometric data are very sensitive to surface condition, so a surface roughness layer was added in the model. A four-layer model (air/ roughness/ $Li_4Ti_5O_{12}$/ substrate) is utilized to describe the $Li_4Ti_5O_{12}$ thin film itself. The surface roughness layer was modeled by Bruggeman effective-medium approximation (EMA) with a mixture of the material (50%) and voids (50%). In order to determine the optical constants of LTO films, the $MgAl_2O_4$ substrate was measured first by ellipsometry. The optical response of the substrate was described using a model of Cauchy to ensure the Kramer-Kronig consistency. Using the information of the substrate, the ellipsometric spectra were evaluated. A Cauchy dispersion model is adopted to describe the optical constants of $Li_4Ti_5O_{12}$ thin film. The expression is given by:

$$n(\lambda) = A + B/\lambda^2 + C/\lambda^4 \tag{2}$$

$$k(\lambda) = D/\lambda + E/\lambda^3 + F/\lambda^5 \tag{3}$$

Where A, B, C, D, E, F are the model parameters. The best fitting parameters of the model is displayed in Table 1. The refractive index decreases slowly with the increase of wavelength according to the Cauchy model in Fig. 3(b). The thickness of the film and the roughness layer are 86.13nm and 4.61nm, respectively.

Optical Materials EXPRESS

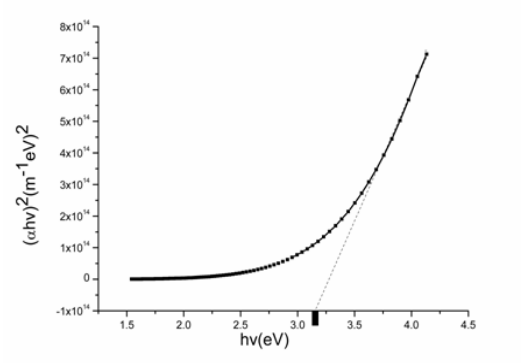

Fig. 4. The relationship between $(\alpha h\nu)^2$ and photon energy $(h\nu)$ known as the Tauc plot for $Li_4Ti_5O_{12}$ thin film.

The optical band gap Eg of the $Li_4Ti_5O_{12}$ film was determined using the extinction coefficient from the following Tauc expression:

$$E - E_g = \left\{ \left(\frac{4\pi\kappa}{\lambda} \right) \frac{h\nu}{B} \right\}^n \tag{4}$$

Where E is the photon energy ($\equiv h\nu$), B is a constant, $\alpha = 4\pi\kappa/\lambda$ is the absorption coefficient and κ is the extinction coefficient. The exponent n depends on the type of optical transition [23]. Depending on the type of electronic transition in bulk semiconductors, the exponent is n = 1/2, 2, 1/3 and 2/3 for indirect allowed, direct allowed, indirect forbidden and direct forbidden transitions, respectively. $Li_4Ti_5O_{12}$ has a direct bandgap, we plotted the curve of $(\alpha h\nu)^2$ vs $h\nu$ and extrapolated the linear segments of the curve to get the optical bandgap. As shown in Fig. 4, the optical bandgap is about 3.14 ± 0.12eV. $Li_4Ti_5O_{12}$ is an insulating nature material, in which the bandgap opens between the occupied O_{2p} valance states and empty Ti_{3d} conduction band. $Li_4Ti_5O_{12}$ is a wide band gap semiconductor and its bandgap value varies widely in the literature. Although our calculated bandgap value significantly exceed the theoretical bandgap values of 2.0eV [24] and 2.3eV [25], there are, nevertheless, reports that the bandgap value of $Li_4Ti_5O_{12}$ is about 3eV [26] and 3.1eV [27], which is in good agreement with our result.

Optical Materials EXPRESS

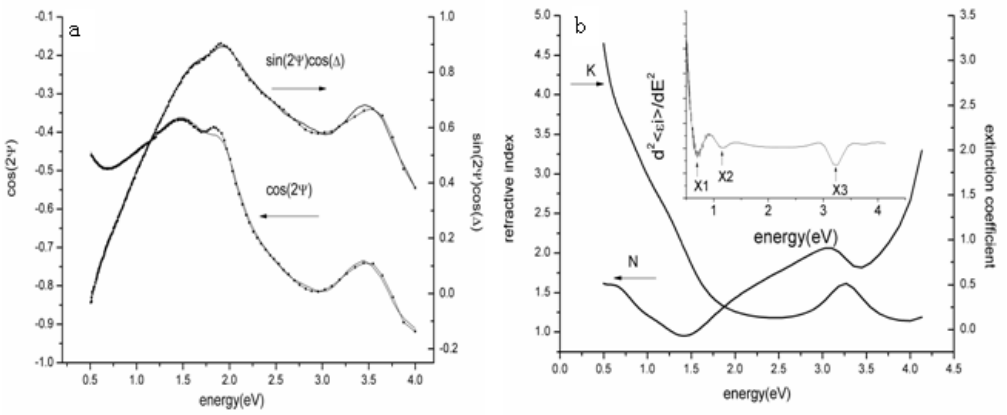

Fig. 5. (a) Measured (line-dots) and fitted (lines) ellipsometric spectra cos(2 ψ) and sin(2 ψ)cos(Δ) of $LiTi_2O_4$ thin film at the incident angle of 75°(b) Refractive index and extinction coefficient shown for $LiTi_2O_4$ thin film at room temperature, the inset shows the second derivative of extinction coefficient.

Table 2. The best fitting parameters in the Lorentz oscillators and Drude model for the $LiTi_2O_4$ film.

Lorentz		A	L_0 (um)	ϒ
	Peak 1	4.018705	1.655550	1.573365
	Peak 2	0.674966	1.057313	0.633824
	Peak 3	0.331477	0.379688	0.064937
	Peak 4	0.856379	0.286395	2.6694E-3
Drude		P	B	C
		2.332912	0.176578	1.696921

In contrast to $Li_4Ti_5O_{12}$, the valence bands of $LiTi_2O_4$ are mainly composed of the O_{2p} states, with partial contributions from Ti_{3d} orbits. The conduction bands are primarily assigned to the Ti_{3d} states, and the partially filled Ti_{3d} states cause $LiTi_2O_4$ possessing metallic characteristics [28–31]. Ellipsometry data of $LiTi_2O_4$ from 0.496 to 4.13eV (300-2500nm) are shown in Fig. 5(a). By introducing the Drude-Lorentz dispersion model to describe the optical constants of $LiTi_2O_4$ thin film, the simulated spectra are in excellent agreement with the measured spectra. The result of optical constants confirms that the spinel $LiTi_2O_4$ is a metallic compound. The Drude-Lorentz dispersion model is given by:

$$\text{Drude: } \varepsilon_r = P - C^2 * \lambda^2 / (1 + (\lambda * B)^2) \tag{5}$$

$$\varepsilon_i = B * C^2 * \lambda^3 / (1 + (\lambda * B)^2) \tag{6}$$

$$\text{Lorentz: } \varepsilon_r = A * \lambda^2 * (\lambda^2 - L_0^{\,2}) / \left[(\lambda^2 - L_0^{\,2})^2 + \gamma^2 * \lambda^2 \right] \tag{7}$$

$$\varepsilon_i = A * \lambda^3 * \gamma / \left[(\lambda^2 - L_0^{\,2})^2 + \gamma^2 * \lambda^2 \right] \tag{8}$$

where P is the polarization; B and C are the mean free path and the inverse of the plasma wavelength, respectively; A, L_0, γ introduce the intensity, the central wavelength and the width of the peak of Lorentz oscillator. A four-layer model (air/ roughness/ $LiTi_2O_4$/ substrate) is used in this situation. To obtain more precise optical constants of $LiTi_2O_4$, the influence of the roughness layer is eliminated. The surface roughness layer was described by

Optical Materials EXPRESS

Bruggeman effective-medium approximation (EMA) with a mixing fraction of 50%, and the thickness of roughness layer is fixed as 1.3nm (originated from AFM test). The best fitting parameters are listed in Table 2, and the thickness of $LiTi_2O_4$ thin film is 194.8nm. Fig. 5(b) displays the optical constants of $LiTi_2O_4$ at room temperature as a function of energy, and the inset shows the second derivative spectra of extinction coefficient derived from the numerical calculation of the corresponding optical constants. In the spectrum of the second derivative of extinction coefficient, we can observe that optical transitions labeled X1, X2 and X3 are located at about 0.74eV, 1.17eV and 3.26eV, respectively.

The interband transitions in spinel material are very complex, mainly originate from three types of electronic transition process: intervalence charge transfer (IVCT) transitions, intersublattice charge transfer (ISCT) transitions, crystal field (CF) transitions. IVCT transitions are transitions in which an electron, through optical excitation, is transferred from one cation to a neighboring cation. When the two cations are on different crystallographic sites, IVCT transitions are traditionally called ISCT transitions. CF transtions is a single-ion transition, while the former two transitions involve two cations. For normal spinel materials $CoFe_2O_4$, the absorption feature at 0.83eV corresponds to a CF transition within the spin state of tetrahedrally coordinated Co^{2+} ions, namely between $^4A_2$ and $^4T_1$ bands, Co^{2+} on A site, as reported by Fontijn et al [32]. The tetrahedral sites in $LiTi_2O_4$ are occupied by lithium ions. The behaviour of Li^+ is similar to Co^{2+}, so we attribute the X1 feature located below ~1eV to the CF transitions between $^4A_2$ and $^4T_1$ bands, which represent the ground state and the excited states, respectively, according to standard crystal-field theory [33]. The broad structures X2 and X3 are interpreted as being contributed by two similarly transitions, namely CT transitions involving O^{2-} and octahedral Ti^{3+}/Ti^{4+} ions, ie., $O^{2-}(2p) \rightarrow Ti^{3+}/Ti^{4+}(3d)$ for 1.17 (t_{2g}) and 3.26eV (e_g) structures, similar to spinel $LiNi_xMn_{2-x}O_4$ reported by Kim [34]. The Ti_{3d} orbitals are split by the cubic component of the crystal field into t_{2g} orbitals and e_g orbitals. The t_{2g} band is half-filled while the higher-lying e_g band is empty. The broader nature of the t_{2g} energy-band width compared to the e_g band [30] is reflected in the broader Lorentz oscillator parameter γ shown in Table 2. From the difference between the energies of the CT transitions (X2, X3), the energy splitting between the t_{2g} and the e_g orbitals was calculated to amount to 2.09eV. For the ideal cubic spinel structure, the splitting energy gap between t_{2g} and the e_g orbitals is about 1.36eV [29]. However, for the real structure, a small octahedral distortion leads to a broadening of the gap and the value extends to 2.28eV [30]. Our calculated value of the gap is a little smaller than the theoretical reported value. The difference is in the acceptable range.

4. Summary

$Li_{1+x}Ti_{2-x}O_4$ with x = 0 and x = 1/3 thin films were deposited onto $MgAl_2O_4$ substrates by plused laser deposition, and their optical constants were derived using spectroscopic ellipsometry. Good model fits for $Li_4Ti_5O_{12}$ and $LiTi_2O_4$ were achieved using Cauchy dispersion model and Drude-Lorentz dispersion model, respectively. The analysis of the extinction coefficient of $Li_4Ti_5O_{12}$ indicates a wide bandgap of about 3.14eV. To the best of our knowledge, the optical constants of $LiTi_2O_4$ was observed for the first time, and we try to explain interband transtitions of normal state of $LiTi_2O_4$. The crystal-field splitting between the e_g and the t_{2g} states of the octahedral Ti^{3+}/Ti^{4+} ion estimated from the assigned charge transfer transitions is about 2.09eV.

Funding

National Key Basic Research Program of China (2015CB921003) and the Fund grants No.2016JC027.

Optical Materials EXPRESS

Acknowledgments

M. L. Zhao acknowledges the assistance from Ge He and Yujun Shi for proofreading and useful discussion.